ISBN: 978-3-95450-249-3 ISSN: 2673-5350 doi: 10.18429/JACoW-IBIC2024-TUBC4

BEAM SIZE MEASUREMENT WITH GRATINGS AT BEPCII*

Wan Zhang†, Dechong Zhu[1], Yanfeng Sui[1], Junhui Yue[1], Jianshe Cao[1], Jun He[1], Institute of High Energy Physics, Chinese Academy of Sciences, Beijing 100049, China
[1]also at University of Chinese Academy of Sciences, Beijing 100049, China

Abstract

The vertical beam size measurement was carried out at BEPCII using a phase grating and an absorption grating based on the Talbot effect. Due to the partial coherence of the source, coherence length can be calculated by measuring the visibility decay of interferograms recorded at different distances behind gratings. The vertical beam size of 68.19±2 μm was obtained based on the relationship between coherence length and source size. A comparison of the vertical emittance derived from grating Talbot method and synchrotron radiation visible light interferometer method was presented to evaluate the method. The vertical emittances from two methods are 1.41 nm·rad and 1.40 nm·rad, respectively. The 0.1% difference indicates the grating Talbot method for beam size measurement is reliable. This technique has great potential in small beam size measurement in the fourth-generation synchrotron radiation light source, considering its small diffraction limitation and simple experimental setups.

INTRODUCTION

The requirements of synchrotron radiation facilities about high coherence, high brightness and small beam sizes have been proposed in some x-ray beamlines for applications such as x-ray phase contrast imaging, coherent x-ray diffraction imaging and x-ray holography [1-3]. The beam size measurement is essential for beam adjustment and beam dynamics study.

Synchrotron light can afford to measure beam sizes in synchrotron radiation facility [4, 5]. Thanks to its short wavelength, x-ray can greatly improve the imaging resolution to meet small beam size measurements. The x-ray pinhole imaging, as a common method, has been applied at Diamond Light Source (DLS), European Synchrotron Radiation Facility (ESRF) and so on [6-8]. It is characterized by real-time and high measurement accuracy. However, it doesn't work for extremely small beam size due to low resolution caused by diffraction limitation and imaging. X-ray Fresnel zone plates (FZP) imaging and KB mirror focusing imaging show advantages in micron-scale beam size measurement. However, they suffer from high processing difficulties [9, 10]. In recent years, some new measurement systems have been established for beam size measurement. [11, 12].

For the case of synchrotron radiation sources with high coherence, it is feasible to derive light source size by spatial coherence. One of the Talbot effect applications is focused on spatial coherence measurements of x-ray in synchrotron radiation sources. The spatial coherence of x-ray emitted from a bending magnet has been measured using the Talbot effect of a π/2 phase checkerboard grating and a π/2 phase circular grating respectively at Advanced Photon Source (APS) [13, 14]. However, the above articles are of no interest to beam size measurement. Given the relationship between spatial coherence and source size, the grating Talbot method can afford to measure beam size owing to its little diffraction limitation. Most importantly, the experimental setup is simple, which only needs gratings, a displacement platform, and an x-ray camera without changing any components in the beamline front end.

At BEPCII, we measured the vertical beam size at 3W1 beamline employing the grating Talbot effect. A partially coherent quasi-monochromatic x-ray has been employed in this experiment. The vertical beam size is calculated successfully from the self-image interference fringes of a grating interferometer. Then the vertical emittance of the storage ring is calculated by the vertical beam size and β function. The vertical emittance from a bending magnet is derived using visible light interference method. An extremely small difference between the two vertical emittances is presented, which illustrates that the grating Talbot effect method is of great potential to measure beam size.

THEORY BACKGROUND

In 1836, Talbot found that a monochromatic parallel beam transmitting through a grating vertically will generate a series of grating images at certain distances behind the grating, which is called Talbot effect [15]. There is a specific relationship between the visibility of the Talbot image and the complex coherence function of the light source [16, 17].

The interference intensity of two beams from an extended source at any point can be written as

$$\begin{aligned} \mathrm{I} &= \langle [E(p_1)+E(p_2)]\,[E^*(p_1)+E^*(p_2)] \rangle \\ &= I_1 + I_2 + 2Re\{J_{12}\} \end{aligned} \quad (1)$$

where E(p_1) and E(p_2) are electric fields formed by two points on an extended source, and J_{12} is the mutual intensity function of the two light beams from the two points [18].

The normalized mutual intensity function j_{12}, called the complex coherence function, is expressed as

$$j_{12} = \frac{J_{12}}{\sqrt{J_{11}J_{22}}} = \frac{J_{12}}{\sqrt{I_1 I_2}} \quad (2)$$

Combining Eq. (1) and Eq. (2)

$$\mathrm{I} = I_1 + I_2 + 2\sqrt{I_1 I_2}|j_{12}|\cos(\varphi_{j_{12}}) \quad (3)$$

where φ_{j12}=Arg(j_{12}). The third term of Eq. (3) expresses the interference effect. $|j_{12}|$ takes the value 1 corresponding to the complete coherence of the two beams and takes the value 0 corresponding to the complete incoherence. In the case of partial coherence, it takes value between 0 and 1.

* Work supported by The Youth Innovation Promotion Association CAS (award No. Y202005).
† email address: zhangwan@ihep.ac.cn

ISBN: 978-3-95450-249-3 ISSN: 2673-5350 doi: 10.18429/JACoW-IBIC2024-TUBC4

The complex coherence function can be calculated from the visibility measurement of interference fringes formed by two light beams. The visibility can be expressed as

$$V = \frac{I_{max}-I_{min}}{I_{max}+I_{min}} \quad (4)$$

where I_{max} and I_{min} are the maxima and minima intensity of interference fringes respectively. They can be achieved from Eq. (3),

$$I_{max} = I_1 + I_2 + 2\sqrt{I_1 I_2}|j_{12}|, I_{min} = I_1 + I_2 - 2\sqrt{I_1 I_2}|j_{12}| \quad (5)$$

Inserting Eq. (5) into Eq. (4),

$$|j_{12}| = \frac{V(I_1+I_2)}{2\sqrt{I_1 I_2}} \quad (6)$$

For a phase grating, I_1=I_2, Eq. (6) can be rewritten as

$$|j_{12}| = V \quad (7)$$

That is to say, the visibility of fringes is equal to the coherence degree of beam.

The synchrotron radiation intensity has a good approximation of Gaussian distribution, which can be written as

$$I_s(s_x, s_y) = I_0 exp\left[-\frac{s_x^2}{2\sigma_x^2} - \frac{s_y^2}{2\sigma_y^2}\right] \quad (8)$$

where s_x, s_y are the coordinates in the source plane, σ_x and σ_y are the source size along horizontal and vertical directions, respectively.

The complex coherence function is also a Gaussian distribution according to the propagation theory of mutual intensity function, which is expressed as

$$|j(x,y)| = j_0 exp\left[-\frac{x^2}{2\xi_x^2} - \frac{y^2}{2\xi_y^2}\right] \quad (9)$$

$$\xi_x = \frac{\lambda D}{2\pi\sigma_x}, \xi_y = \frac{\lambda D}{2\pi\sigma_y} \quad (10)$$

where x and y are the horizontal and vertical axes which are perpendicular to the direction of beam propagation, ξ_x and ξ_y are the coherence length in x and y directions, respectively, D is the beam propagation distance from the source, and λ is the transmission wavelength.

In this experiment, the measured visibilities are from a series of grating self-imaging interference fringes at different d, the distance between grating and camera. For a $\pi/2$ phase-shift grating, the interference fringes are formed by the neighbouring diffraction orders, thus the coordinates in Eq. (9) can be rewritten in terms of d [18],

$$i = \frac{d\lambda}{p_i}, i = x, y \quad (11)$$

where p_i is the period of interference fringes along i direction. As a consequence, Eq. (9) can be expressed as a function of d

$$|j(d)| = j_0 \exp\left(\frac{-d^2}{2*(\delta_i)^2}\right) \quad (12)$$

where δ_i is the width of Gaussian envelop function along i direction. Combining Eq. (9) and Eq. (11), the coherence length can be expressed as

$$\xi_{exp,i} = \frac{\lambda\delta_i}{p_i}, i = x, y \quad (13)$$

Inserting the measured coherence length $\xi_{exp,i}$ to Eq. (10), the source size can be calculated.

EXPERIMENTAL SETUP

Figure 1 shows the schematic of the experimental setup. A 9×1.3 mm^2 slit is placed 15.54 m from the source. The double-crystal monochromator (DCM), consisting of two Si(311) crystals, is located downstream of the silt 2.25 m. The output photon energy of 15 keV is obtained using tuning DCM. The x-ray energy bandwidth is (1.7±0.001)×10^{-5}. A beryllium window is 9.48 m away from DCM. The 1-D $\pi/2$ phase grating with a period of 2.4 μm is placed 28.91 m from the source. The 1-D absorption grating with the same period is placed close to the x-ray camera to detect clear interference fringes at different distances d. The x-ray camera consists of a CCD, a lens and a LYSO (lutetium-yttrium oxyorthosilicate) scintillator which is used to convert x-rays into visible light. The CCD pixel size is 6.5×6.5 μm^2 and the lens magnification is 20. The resolution of the x-ray camera is about 0.65 μm, which is sufficient to detect the self-imaging fringes of the grating interferometer.

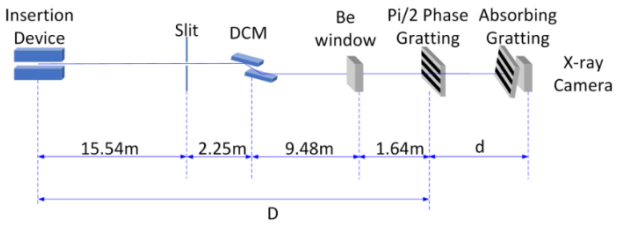

Figure 1: The schematic of experimental setup.

The grating interferometer consists of a phase grating and an absorption grating. Figure 2 shows the pictures and scanning electron microscope images of two gratings fabricated by Microworks, Germany. The black line in the picture indicates the direction of grating lines. Some fabricating parameters of gratings are shown in Table 1. Considering the beam size and the distance between the source and gratings, the gratings period of 2.4 μm has been selected. The duty cycle is set as 0.5 for uniform self-imaging fringes. The polymer height of phase grating 18.6 μm and the gold height of absorption grating 14 μm are determined by phase shift and x-ray energy of 15 keV.

The experimental grating interferometer is shown in Figure 3. The phase grating is fixed on an optical platform. The absorption grating and x-ray camera move together along the direction of light propagation. The phase grating produces self-images at fractional Talbot distances (dn) following the equation d_n=n*(p2/2λ), where n=0.5, 1.5, 2.5…[19]. Each self-image is superimposed with absorption grating forming Moire fringe which is detected by an x-ray camera. The grating lines are placed horizontally for the measurement of vertical beam size.

Table 1: Some Fabricating Parameters of Gratings

Parameters	phase grating	absorption grating
Period	2.4 μm	2.4 μm
Duty Cycle	0.53±0.01	0.51±0.01
Area	>2.5×2.5 mm^2	>2.5×2.5 mm^2
Height	Polymer 18.6 μm	Gold 14±1 μm
Substrate	10 μm Polyimide	10 μm Polyimide

ISBN: 978-3-95450-249-3 ISSN: 2673-5350 doi: 10.18429/JACoW-IBIC2024-TUBC4

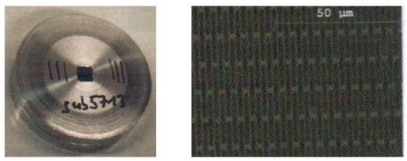

(a) phase grating

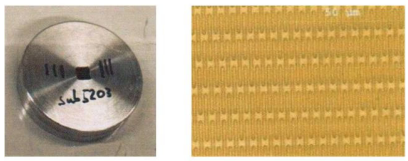

(b) absorption grating

Figure 2: The pictures and scanning electron microscope images of (a) phase grating and (b) absorption grating.

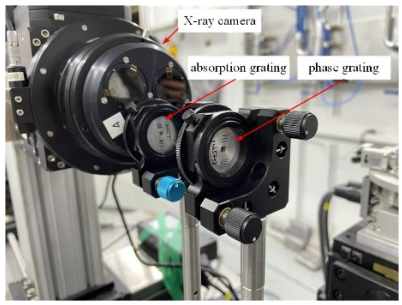

Figure 3: The experimental grating interferometer.

RESULTS AND ANALYSIS

The interferograms at multiple detection positions from 40 mm (close to the phase grating) to 410 mm (the maximum distance) with an interval of 4 mm are presented. The visibility of each interferogram as a function of detection distance d is shown in Figure 4. As expected, the visibility shows periodic oscillations and the local maximum of visibility at fractional Talbot distance decreases gradually due to the partial coherence of the source. The envelope function drawn through these maximum visibility points is Gaussian.

Figure 5 shows the fitted Gaussian envelope curve drawn through the maximum visibility points. The visibility error bars are introduced through multiple measurements. The first fractional Talbot distance about 34 mm is eliminated, since it is smaller than the minimum distance between two gratings. The R^2 of the fitted Gaussian function is greater than 0.99, presenting a high fitting accuracy. The width of envelope function σ is 162.03±4.6 mm. The transverse coherence of the x-ray can be calculated by utilizing the width of the envelope function according to the theory in part 2. The vertical coherence length of 5.58±0.16 μm on the phase grating plane is achieved. The vertical beam size calculated by inserting vertical coherence length into Eq. (10) is σ_y=68.19±2 μm.

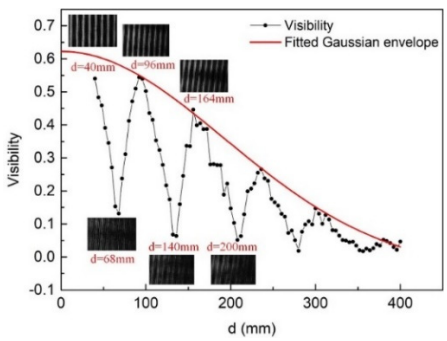

Figure 4: The visibility as a function of detection distance d.

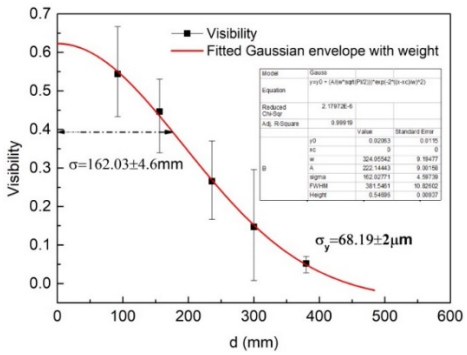

Figure 5: The fitted Gaussian envelope curve drawn through the maximum visibility points.

The vertical emittance ε_y is a constant for an accelerator. It can be calculated by vertical beam size and Lattice parameter β_y at the source point according to the formula $\sigma_y^2=\varepsilon_y\beta_y$. The experimental results are assessed through comparing two vertical emittances from two methods, the grating self-imaging method (at 3W1 beamline with wiggler source) and synchrotron radiation (SR) interferometer method (at visible light beamline with bending magnet source).

At the visible light beamline of BEPCII, we measured the vertical beam size by a double-slit interferometer with a wavelength of 550 nm. Because of measurement error, the spatial coherence should be in the range of 0.1~0.9. Taking into account the relationship of light intensity, single slit width and double-slit distance, the slit width of 0.8 mm and the double-slit distance of 4 mm are selected. The distance from double-slit to detector R is 0.5 m. Figure 6 shows the interference fringes collected in the vertical beam size measurement experiment. By fitting the curve, the vertical beam size of 172 μm is derived.

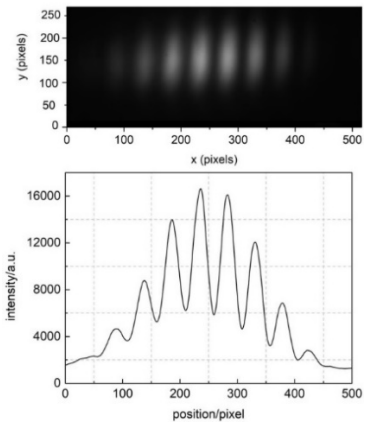

Figure 6: The interference fringes and the intensity distribution curve for vertical beam size measurement.

ISBN: 978-3-95450-249-3 ISSN: 2673-5350 doi: 10.18429/JACoW-IBIC2024-TUBC4

The vertical emittances from two methods are presented. β_y is 3.29 m and 20.98 m of 3W1 beamline source and visible light beamline, respectively. According to the formula $\sigma_y^2=\varepsilon_y\beta_y$, the measured vertical emittance is 1.41 nm·rad at 3W1 beamline and 1.40 nm·rad at visible light beamline. The extremely small difference between the two values, about 0.1%, indicates that the grating self-imaging method can afford to measure beam size in a synchrotron radiation source.

Possible future measurements for smaller beam sizes of the fourth-generation synchrotron light sources with higher light source coherence are being considered due to the little diffraction limitation and simple experimental setups of the proposed method.

CONCLUSION

A method based on the grating self-imaging effect for the partial coherence of the x-ray, the transverse coherence of the beam wavefront has a relationship with the visibility of self-imaging interferograms. The beam size can be derived from transverse coherence.

In this paper, the vertical beam size from a wiggler source is measured by extracting visibilities of interferograms formed by phase grating self-images and absorption grating. The interferograms, also called Moiré fringe, has a larger fringe period and are conducive to visibility extraction. The transverse coherence of 5.58±0.16 μm at the vertical direction in the plane of phase grating is obtained from the width of the fitted Gaussian envelope function. Then the vertical beam size is calculated to be 68.19±2 μm. Finally, to evaluate the accuracy of experimental results, the vertical emittances derived from the grating self-imaging method and SR interferometer method are compared, which are 1.41 nm·rad and 1.40 nm·rad respectively. Thanks to the extremely small difference, about 0.1%, the grating self-imaging method for measuring beam size is considered to be reliable and accurate. This technique will have great prospects for application in small beam size measurement of the fourth-generation synchrotron light sources, benefiting from the little influence of diffraction limitation.

ACKNOWLEDGEMENTS

This work was performed in BEPCII, Institute of High Energy Physics, Chinese Academy of Sciences, Beijing 100039, China. The authors would like to thank and acknowledge Yiming Yang, Lirong Zhen, Gang Li, Jie Zhang from beamline at BEPCII for their assistance during the experiment preparation.

REFERENCES

[1] D. K. Pogoreliy *et al.,* "Real-time phase-contrast imaging at the Kurchatov synchrotron radiation source", *Nucl. Instrum. Methods,* vol. 603, pp. 167-169, 2009. doi:10.1016/j.nima.2008.12.146

[2] W. Yang *et al.,* "Coherent diffraction imaging of nanoscale strain evolution in a single crystal under high pressure", *Nat. Commun.,* vol. 4, p. 1680, 2013. doi:10.1038/ncomms2661

[3] A. Sakdinawat and D. Attwood, "Nanoscale X-ray imaging", *Nat. Photonics*, vol. 4, no. 12, pp. 840-848, 2010. doi:10.1038/nphoton.2010.267

[4] A. D. Garg *et al*., "Design of synchrotron radiation interferometer (SRI) for beam size measurement at visible diagnostics beamline in Indus-2 SRS", *Nucl. Instrum. Methods*, vol. 902, pp. 164-172, 2018. doi:10.1016/j.nima.2018.06.024

[5] T. Mitsuhashi, "Beam profile and size measurement by SR interferometers", in: Proceedings of the Joint US–CERN–Japan–Russia School on Particle Accelerators, World Scientific, Montreux and Geneva, Switzerland, 1999, pp. 399-427. doi:10.1142/9789812818003_0018

[6] C. Thomas, G. Rehm, and I. Martin, "X-ray pinhole camera resolution and emittance measurement", *Phys. Rev. Spec. Top-AC.*, vol. 13, no. 022805, 2010. doi:10.1103/PhysRevSTAB.13.022805

[7] A. Garg *et al*., "Design of x-ray diagnostic beamline for a synchrotron radiation source and measurement results", *Nucl. Instrum. Methods Phys. Res. A*, vol. 754, pp. 15-23, 2014. doi:10.1016/j.nima.2014.04.013

[8] W. Leitenberger *et al*., "Double pinhole diffraction of white synchrotron radiation", *Physica B*, vol. 336, pp. 63-67, 2003. doi:10.1016/S0921-4526(03)00270-9

[9] Y. Suzuki *et al*., "X-ray microbeam with sputtered-sliced Fresnel zone plate at SPring-8 undulator beamline", *Nucl. Instrum. Methods*, vol. 467, pp. 951-953, 2001. doi:10.1016/S0168-9002(01)00532-0

[10] A. Alatas *et al*., "Improved focusing capability for inelastic X-ray spectrometer at 3-ID of the APS: A combination of toroidal and Kirkpatrick-Baez (KB) mirrors", *Nucl. Instrum. Methods*, vol. 649, pp. 166-168, 2011. doi:10.1016/j.nima.2010.11.068

[11] N. Samadi, X. Shi, L. Dallinc, and D. Chapmanc, "A real-time phase-space beam emittance monitoring system", *J. Synchrotron Rad*., vol. 26, pp. 1213-1219, 2019. doi:10.1107/S1600577519005423

[12] Y. Kagoshima *et al*., "Measurement of the horizontal beam emittance of undulator radiation by tandem-double-slit optical system", *J. Synchrotron Rad.*, vol. 27, pp. 799-803, 2020. doi:10.1107/S1600577520004415

[13] S. Marathe *et al*., "Probing transverse coherence of x-ray beam with 2-D phase grating interferometer", *Optics Express*, vol. 22, pp. 14041-14053, 2014. doi:10.1364/oe.22.014041

[14] X. Shi *et al*., "Circular grating interferometer for mapping transverse coherence area of X-ray beams", *Appl. Phys. Lett*., vol. 105, p. 041116, 2014. doi:10.1063/1.4892002

[15] M. Born and E. Wolf, "Principles of Optics", 7th ed. University Press, Cambridge, 1999.

[16] P. Cloetens, J. P. Guigay, C. De Martino, J. Baruchel, and M. Schlenker, "Fractional Talbot imaging of phase gratings with hard x rays", *Opt. Lett.*, vol. 22, pp. 1059-1061, 1997. doi:10.1364/OL.22.001059

[17] J. P. Guigay, S. Zabler, P. Cloetens, C. David, R. Mokso, and M. Schlenker, "The partial Talbot effect and its use in measuring the coherence of synchrotron X-rays", *J. Synchrotron*

ISBN: 978-3-95450-249-3 ISSN: 2673-5350 doi: 10.18429/JACoW-IBIC2024-TUBC4

Radiat. vol. 11, no.6, pp. 476-482, 2004. doi:10.1107/S0909049504024811

[18] F. Pfeiffer *et al*., "Shearing interferometer for quantifying the coherence of hard X-ray beams", *Phys. Rev. Lett*., vol. 94, no. 16, p. 164801, 2005. doi:10.1103/PhysRevLett.94.164801

[19] I. Zanette, C. David, S. Rutishauser, and T. Weitkamp, "2D grating simulation for X-ray phase-contrast and dark-field imaging with a Talbot interferometer", *AIP Conf. Proc*., vol. 1221, pp. 73-79, 2010. doi:10.1063/1.3399260